Sustainable Materials and Technologies 41 (2024) e01038

Contents lists available at ScienceDirect

Sustainable Materials and Technologies

journal homepage: www.elsevier.com/locate/susmat

Energy-saving approach for mechanical properties enhancement of recycled PET additively manufactured by MEX

Luca Landolfi [a,b,1], Andrea Lorenzo Henri Sergio Detry [a,*,1], Ersilia Cozzolino [a], Daniele Tammaro [a], Antonino Squillace [a]

[a] Department of Chemical Materials and Production Engineering, University of Naples Federico II, Piazzale Vincenzo Tecchio, 80, Napoli, 80125, NA, Italy
[b] Department of Management, Information and Production Engineering, University of Bergamo, Via Pasubio 7B, Dalmine, 24044, BG, Italy

ARTICLE INFO

Keywords:
Additive manufacturing
Material extrusion
Bottle recycling
Optimal parameter
Multivariate DOE

ABSTRACT

This study investigates the recycling of polyethylene terephthalate (PET) water bottles by material extrusion (MEX), an additive manufacturing (AM) technique, with a focus on characterising energy consumption and mechanical properties throughout the recycling process. The process encompasses shredding of the bottles, filament production, and the printing of tensile specimens. A full factorial design of experiment (DoE) was used to investigate the impact of various process parameters on product quality from an energy-saving perspective. The results provide important insights into energy efficiency and mechanical performance, identifying the optimal production conditions that balance environmental sustainability and material functionality. The results show that by optimizing printing parameters, energy consumption can be reduced by up to 30%, while the tensile strength of the printed samples can be increased by 20%. This research contributes to a broader understanding of the potential for AM in PET recycling, providing a pathway towards more localized and sustainable manufacturing practices.

1. Introduction

1.1. Background

The need for sustainable practices has never been more critical in the face of increasing environmental challenges such as climate change, overconsumption, population growth and unchecked economic development [1–3]. In this context, sustainability represents a development paradigm that not only meets the needs of the present, but also safeguards the prospects of future generations. The advent of Additive Manufacturing (AM) has opened new avenues for recycling and material innovation [4], particularly in the realm of polymers [5]. Polyethylene Terephthalate (PET) was selected for this research due to its widespread use in consumer packaging and its consequent local availability. This widespread availability highlights the need to develop accessible, low-cost recycling methods for PET, which can significantly reduce both the environmental and economic costs associated with waste transport. PET is a semi-crystalline material, which makes it suitable for a variety of applications. AM is revolutionising manufacturing by creating complex shapes from digital designs, reducing waste and promoting sustainability. It enables the use of a wide range of materials, including polymers like PET, fostering innovation in recycling and material reuse [6]. Indeed, recycled PET contributes to the development of the circular economy. It can be used in producing new bottles, fibers for clothing, packaging strips, pellets, films, and other products. This approach results in the minimization of waste, increasing resource efficiency, and fostering a sustainable economic model. This process aligns with sustainable practices by minimizing material consumption and waste generation, offering a path towards a circular economy [7]. By emphasizing localized production, AM [8–11] reduces the environmental impact of transportation and storage. This highlights its potential to contribute to both environmental sustainability and economic efficiency [12–15].

1.2. Literature review

Recent advancements in Large Format Additive Manufacturing (LFAM) have shown promising avenues for enhancing PET recycling processes. A study from Pintos et al. [16] has highlighted the potential of

* Corresponding author.
E-mail address: andrea.detry@unina.it (A.L.H.S. Detry).
[1] Authors contributed equally

https://doi.org/10.1016/j.susmat.2024.e01038
Received 18 April 2024; Received in revised form 8 June 2024; Accepted 2 July 2024
Available online 16 July 2024

using PET in LFAM, focusing on its semi-crystalline nature which has historically complicated processing efforts. The study compares PET with PETG, a fully amorphous variant with inferior mechanical properties, and identifies a specific PET grade 3 (PET3) that demonstrates excellent printability and superior mechanical and thermal properties. This is due to PET3's slow crystallization behavior, making it a desirable material for industrial applications where PETG is insufficient. In their work, Vidakis et al. [17] demonstrated the potential for using recycled PETG in consecutive 3D printing manufacturing processes. Moreover, Vidakis et al. [18] also demonstrated that Polyamide 12 (PA12) can be successfully recycled for a certain number of courses and could be utilized in 3D printing while exhibiting improved mechanical properties and thermal stability, when compared to virgin material that PA12, thus resulting in a viable option for circular use and 3D printing. These insights provide a promising approach to integrating recycled PET into sustainable manufacturing practices, utilizing the benefits of AM to tackle environmental issues. Within the literature on recycled PET in AM, several key studies can be highlighted. The majority of them investigate the optimization of AM process conditions on part quality [19–23].

For instance, Lui et al. [24] focused on the distributed recycling of PLA waste using granule-based material extrusion, examining the effects of multiple recycling cycles on mechanical performance and material properties. This study revealed consistent decreases in tensile strength, melting temperature, and rheological properties with each recycling cycle, underscoring the limitations of current recycling methodologies in preserving material quality over time. Another work from Schneevogt et al. [25] examined the mechanical potential of recycled PET in fused deposition modeling, aiming to enhance sustainability in 3D printing by comparing recycled and conventional materials. The study explored the sustainability implications and mechanical performance differences between recycled PET and conventional PETG, indicating a critical area for further investigation in terms of material selection for sustainable manufacturing practices. A review on the processing of semi-crystalline polymers in MEX from Vaes et al. [26] highlighted the unique challenges and opportunities presented by these materials, including their impact on crystallinity, mechanical performance, and general part quality. Improving PET recycling processes requires addressing governance challenges in addition to technological advancements. According to Gothár et al. [27], systemic perspectives and governance interventions are necessary to enhance circularity. The authors suggest that comprehending the market relationships and leverage points within the PET recycling network is crucial for implementing effective circular economy initiatives. Furthermore, studies by Vidakis et al. [28] on MEX 3D printing with PA6, PLA, and polycarbonate highlight the importance of multi-objective optimization to balance mechanical properties and energy consumption. These studies use robust experimental designs to find optimal parameter settings, emphasizing the need to balance energy efficiency with mechanical performance in AM.

1.3. Objective

These studies above mentioned collectively reveal a critical gap in the literature: the need for a comprehensive, multi-objective approach that simultaneously considers energy consumption, recycling efficiency, and the mechanical and thermal properties of recycled materials in AM. The present research aims to bridge this gap by providing a holistic view that encompasses all these aspects, thereby contributing to a more sustainable and efficient recycling and manufacturing process. This analysis aims to identify trade-offs between these factors through quantitative analysis, while also seeking to extend the lifecycle of PET materials. Thus, it aims to fill the gap of knowledge existing in the literature in this regard. By contributing to the circular economy, this strategy transforms waste into valuable products directly on-site, reducing reliance on virgin resources and diminishing the environmental impact of polymer waste. Enabling good practices for on-site recycling in laboratories with minimal equipment requirements could lead to a reduction in the environmental footprint. By avoiding the energy-intensive processes and carbon footprint associated with transportation and traditional recycling methods, this approach offers a practical way to directly reuse commonly utilized plastic bottles at their point of origin. This research is driven by a comprehensive approach to enhance PET recycling and reuse via AM, in harmony with overarching sustainability goals. Emphasizing the benefits of on-site recycling, the goal is to introduce a scalable and eco-friendly methodology that transforms the widespread presence of plastic waste into a valuable input for novel manufacturing practices. This initiative seeks to leverage the abundant availability of discarded plastics, reimagining them as a resource for creating new products, thereby contributing to a more sustainable and circular economy. In this study, extrusion temperature, plate temperature and printing speed were varied in ranges recommended by the literature to investigate their influence on both energy consumption and mechanical properties, which were jointly investigated. Indeed, the best compromise to print recycled PET parts that have appreciable mechanical and thermal properties while minimizing energy consumption is investigated. The multiobjective purpose of this study is to find the optimal trade-off between part quality and minimization of energy consumption, which actually represents the novelty introduced throughout this work. In fact, PET is among the most recycled thermoplastics worldwide. It has unique properties, including thermal and chemical stability and stiffness. Moreover, the use of PET waste for producing 3D printing filament represents an opportunity for economic and environmental sustainability [29]. This study aims to release guidelines in the 3D printing of recycled PET by minimizing energy consumption without sacrificing mechanical properties. All the results can find an immediate application in numerous industry fields, such as packaging fabrics, films, molded parts of automotive, and electronics.

2. Materials and methods

This study focuses on a polymer mechanical recycling technique commonly used, that involves three steps: a shredding process to reduce them to smaller fragments (flakes), an extrusion process to create a filament, and a 3D printing process to manufacture the specimens. The process begins with the shredding of PET bottles into small flakes. These flakes are then processed by an extruder to produce filaments. Finally, these filaments are used to manufacture the 3D-printed specimens. Fig. 1 provides a comprehensive overview of the PET recycling process adopted in this study, starting from the raw material to the final product.

2.1. Shredding and filament production

For the filament production in this study, PET bottles from the LETE brand were sourced due to their widespread availability and standard-

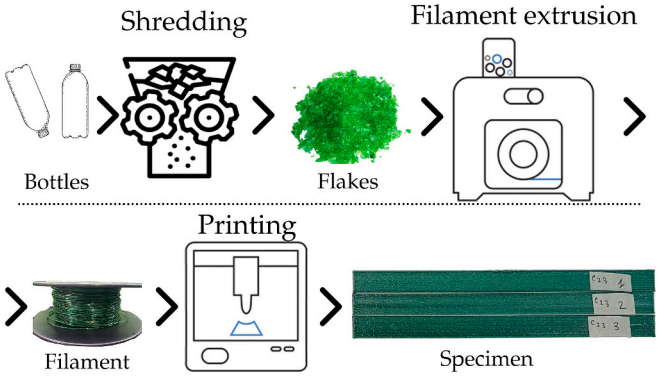

Fig. 1. The process flow of recycling PET bottles into 3D printed specimens: shredding, filament extrusion, and printing.

ized quality, which is crucial for ensuring uniformity in the recycling process. The shredding process transformed the PET bottles into flakes. The bottles were cut into appropriate sizes for the shredder hopper ($20mm < S < 40mm$) and then dried at 150°C for five hours to reduce moisture content. The Felfil Shredder (Felfil, Italy) was used to shred the bottles into flakes. Sieves, designed and produced using a self-built 3D printer, ensured that the flakes met the size requirements for the subsequent extrusion process $0.4mm < D < 4mm$. The flakes were dried at 170°C for six hours before extrusion. The 3DEVO Composer 350 extruder (3DEVO, The Netherlands) produced R-PET filaments with the parameters shown in Table 1, resulting in consistent and high-quality filament with a diameter of $\phi = 1.75 \pm 0.8$ mm.

2.2. 3D printing

All the specimens were manufactured in a single completely automated 3D printing process. Using a custom made filament MEX printer denominated as Step 2.1 that is equipped with a commercial hot end the Vulcano from E3D with a nozzle of 0.6 mm.

Layer width, L_w has been fixed equal to 0.71 mm and it refers to the imposed layer width, which needs to be a multiple of the desired total width of the specimen.

Layer height, L_h has been fixed equal to 0.2mm and it refers to the imposed layer height, required to be a multiple of the desired total height of the specimen [30].

The range of printing parameters was chosen by following the best recommended by the literature. Then, they were refined and finally defined under the conditions of printability of specimens and more complex parts during the first printing trials. In particular, during the printing parameter range selection, clogging issues both with extrusion temperatures higher than 280 °C and lower than 240 °C. For speeds above 100 mm s^{-1} have been experienced. For the temperature of the printing plate lower than 40 °C, problems with parts detaching during printing have been observed. Based on these premises, we redesigned the process parameters range to avoid these issues. Then, a full factorial design of experiment (DoE) was designed to systematically study the influence of extrusion temperature (T_e), printing speed (S_p), and plate temperature (T_p) on the energy consumption and tensile properties of the 3D printed specimens, the level of the DOE are reported in the Table 2.

Three levels of T_e = (250, 260, 270)°C. The selected levels represent a typical range of temperatures employed in the processing of PET in MEX.

Four levels of S_p = (40, 60, 80, 100)mm s^{-1}. The selected speeds were employed to examine the influence of varying deposition rates on the quality and mechanical properties of the printed parts, as well as the energy consumption of the printing process.

Two levels of T_p = (40, 80)°C. The selected temperatures represent a low and high range typically used for PET printing, allowing for the analysis of their effects on the mechanical and thermal properties of the printed parts.

The measured variables include the energy consumption, the average mass (m_{avg}), the maximum load (F_{max}), maximum stress (σ_{max}), and the maximum longitudinal elastic modulus (E_{max}) of each specimen.

Table 1
Filament production parameters.

Parameter	Value
T_1(°C)	255
T_2(°C)	245
T_3(°C)	240
T_4(°C)	240
S_e(*rpm*)	12
Fan speed (%)	100

Table 2
Level of the DOE.

Parameter	1	2	3	4
T_e(°C)	250	260	270	X
T_b(°C)	40	80	X	X
S_p(mm s^{-1})	40	60	80	100

2.3. Differential scanning calorimetry (DSC)

The DSC analyses were conducted using a TA Q2000 DSC in an argon atmosphere. The parameters consisted of a heating rate of 2°C min^{-1}, a cooling rate of 5°C min^{-1}, and modulation of ±0.32°C amplitude over a period of 60 s. The glass transition temperature (Tg) and melting temperature (Tm) were determined from the heat capacity component of the DSC curves. Four samples were analyzed under the DSC before and after the tensile testing. The crystalline weight fraction of the materials was determined following the protocol described in Tammaro et al. [31].

2.4. Thermogravimetric analysis (TGA)

Samples around 5mg were heated in a special alumina container that can hold up to 70 μL using a TA Instruments TGA Q5000 for a linear, non-isothermal thermogravimetric analysis (TGA). These experiments were run at a constant gas flow of 25 mL min^{-1} with temperatures increasing from 25°C to 800°C at a rate of 10°C min^{-1}. Nitrogen gas ($N2$) was used to create an inert atmosphere for studying the material thermal decomposition behavior and its recycled forms (i.e., Filament, Printed sample at 275°C and at 285°C). Each experiment was repeated at least three times, and the average results were considered the most representative values.

2.5. Tensile tests

The tensile properties of the printed specimens were assessed using the Quasar 50 universal testing machine from Galdabini. The testing followed ASTM D638 standards, with a consistent test setup and specimen dimension inputs (parallelepiped of 180X13X3.5 mm). The test involved:

- Positioning of the jaws at 100 mm apart.
- Securing the specimen within the jaws.
- Entering actual specimen dimensions into the machine software.
- Manually halting the test after specimen rupture.

The stress, modulus of elasticity, and energy absorbed were calculated from the load and deformation data.

σ_{max} is the engineering maximum tensile stress.
F_{max} is the maximum measured force applied to the specimen.
F_{max} is the maximum longitudinal elastic modulus that was determined from the slope of the linear elastic region of the stress-strain diagram.

Each test was repeated 3 times, and the results reported refer to the average of the 3 measurements.

2.6. Energy consumption

To measure the energy consumption of the machines used throughout the entire recycling process, a power analyzer C.A 8333 Chauvin Arnoux was used. To analyze energy consumption, the connection type and sensor indices were properly selected on the device before the measurements. For this study, the connection of the machines was monophase with neutral, so one current sensor and two tension cables were adopted to measure current and voltage, respectively. In particular, a current sensor AmpFlex A 193 sensor was used, while the tension cables were equipped with crocodile clips. The current index

sensitivity has been set ranging from 100 mA to 100 A, and the sampling period was fixed equal to 1 s.To visualize all the parameters recorded by the instrument, the Power Analyzer Transfer software was used.

3. Results

The following sections discuss the results of this study. In particular, the effect of T_e, S_p, T_p on the thermal and mechanical properties and energy consumption varies throughout the entire recycling process.

3.1. Shredding

The use of a strainer ensures that the amount of pellets to be reprocessed decreases between cycles. This not only minimised the time required to achieve the desired size, but also prevented already shredded pellets of acceptable size from being reprocessed and subjected to mechanical stress again. About 37 bottles were used to obtain 1100 g of PET flakes, with a weight of ±30 g per bottle.

Table 3 presents the mass reduction of material with each cycle, along with the corresponding energy and time consumption. It is worth noting that the first cycle starts with 1100 g of PET bottles, requiring 480 watt-hours of energy. By the sixth cycle, the mass decreases to 160 g, with only 9 watt-hours needed. The histogram in Fig. 2, demonstrates the effectiveness of this method in reducing the mass of materials that require reprocessing, thereby reducing time and energy waste, increasing efficiency over subsequent cycles due to the use of a sized strainer. The energy consumption required to obtain about 1000 g of acceptable size granules is 670 Wh.

3.2. Filament production

During the second stage of recycling, a suitable compromise was found between the extrusion temperatures assigned to each stage and the extrusion speed, which affects the permanency of the flakes inside the extrusion screw, in order to obtain a filament that could be processed in the MEX printer, and the thermal degradation of the polymer. To evaluate the energy consumption of the extruder, the average power and the energy required to reach steady state conditions were calculated.

Fig. 3 shows the electrical power measured from the activation of the extruder to its operation. The extruder takes approximately 7 min to reach steady-state conditions. The region A represents the preheating phase where the extruder power plateaus at 783 W, heating from room temperature to the target temperature. The moment the target temperature is reached is indicated by the red line, which marks the beginning of polymer extrusion as the extruder screw engages. The Region B marks the beginning of the extrusion process that concludes with a steady state of extrusion characterized by a power plateau at 308 W.

3.3. Thermal properties

The work from Van de Voorde et al. [32] analyzes the impact of MEX processing parameters on the crystallinity and mechanical properties of recycled PET. The study shows that the mechanical performance of the material is significantly influenced by the degree of crystallinity.

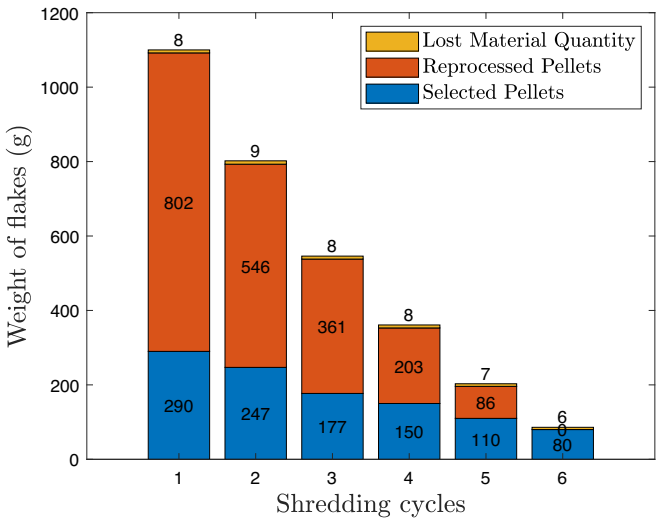

Fig. 2. Efficiency of the PET bottle shredding process over multiple cycles. The histogram depicts the weight distribution of selected pellets, reprocessed pellets, and lost material quantity across six shredding cycles.

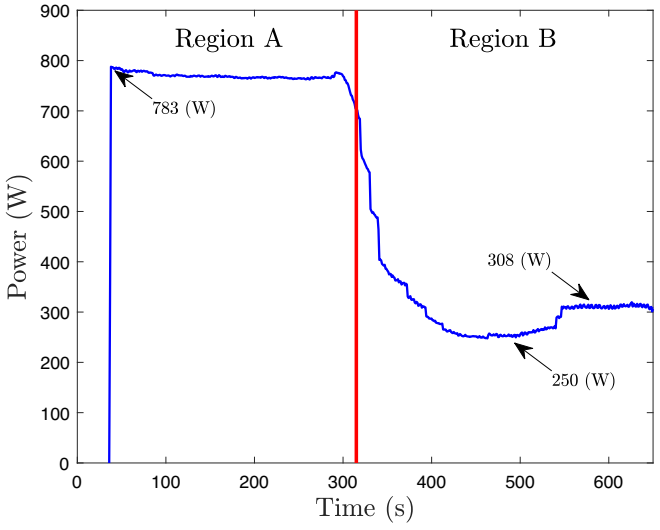

Fig. 3. Power consumption profile of the extruder from start-up to steady-state during PET filament production.

Therefore, it is important to optimize processing conditions to enhance the material's properties. Increasing the deposition speed lead to a higher degree of crystallinity, in Table 4 are shown the results of the calculation of the volumetric flow rate $\left(\dot{Q}_v\right)$ (in the conduct of the extruder with a diameter 2 mm), mean of the residence time (t_r), the Graetz number (G_z) for a family specimen obtained at $T_e = 250$ °C, $T_p = 40$ °C. The definition of the Graetz number, G_z, and the thermal

Table 3
The values of initial weight, time spent, energy spent and average power for each cycle of the shredding process.

Cycle (*No.*)	Mass (g)	Time (*hh* : *mm* : *ss*)	Energy (Wh)	Average Power (W)
1	1100	2:55:40	480	164
2	802	0:33:31	86	154
3	555	0:18:02	46	154
4	378	0:11:05	29	159
5	258	0:6:30	20	166
6	160	0:3:34	9	158

Table 4
Thermal properties of specimen obtained at $T_e = 250$ °C, $T_b = 40$ °C. $\dot{Q}_v$ = volumetric flow rate, t_r = mean of the residence time, G_z = Graetz number, D_{Cb} = degree of crystallinity before tensile test, D_{Ca} = degree of crystallinity after tensile test.

S_p (°C)	$\dot{Q}_v$ (mm^3 s^{-1})	t_r (s)	G_z	D_{Cb} (%)	D_{Ca} (%)
40	11.304	5.56	3.6	15.9 ± 0.6	8.5 ± 0.4
60	16.956	3.70	5.4	22 ± 0.6	11.5 ± 0.5
80	22.608	2.78	7.02	5 ± 0.4	13.5 ± 0.5
100	28.26	2.22	9	10 ± 0.5	14.5 ± 0.6

diffusivity, α, is given by Eq. :

$$G_z = \frac{\dot{Q}_v}{\pi \cdot L \cdot \alpha} \quad ; \quad \alpha = \frac{k}{\rho \cdot C_p} \tag{1}$$

where:

- Q is the volumetric flow rate ($mm^3\ s^{-1}$),
- α is the thermal diffusivity ($m^2\ s^{-1}$),
- $k = 0.3\left(W m^{-1^\circ} C^{-1}\right)$ is the thermal conductivity,
- $\rho = 1.20\left(g\ cm^{-3}\right)$ is the mass density
- $C_p = 1250\left(J\ g^{-1^\circ} C^{-1}\right)$ is the isobaric specific heat capacity.

The Graetz number rises in conjunction with the deposition speed, suggesting a relationship between the thermal and flow dynamics within the extrusion process and the resulting material properties. The results plotted in Fig. 4 confirmed that the degree of crystallinity (D_c) increased with the deposition speed, a phenomenon attributed to the decreased melting time available for the crystals.

The analysis of crystallinity was performed in the specimens after the tensile test (orange dot in Fig. 4) showing a trend that does not follow a defined pattern. This observation can be attributed to a phenomenon known as deformation-induced crystallization [33] occurring in the specimens after tensile testing. In the four examined samples, not only does the deposition speed change, but also the deformation induced by the tensile test varies from sample to sample. This variation could obscure the crystallinity of the starting material.

The weight loss data obtained through TGA for PET are presented in Fig. 6. The Figure shows the data obtained under an inert atmosphere of nitrogen gas (N2), allowing observation of the thermal decomposition behavior of PET and its recycled forms.

The thermal decomposition of PET happened in a single stage, regardless of how many times it was reprocessed. The material showed high stability up to around 380°C. Then, it decomposed rapidly between 380°C and 480°C, losing most of its mass. After that, the remaining material continued to decompose steadily until the end of the experiment. Interestingly, the amount of mass lost remained nearly constant with each reprocessing cycle, such as extrusion and printing. This suggests that the reprocessing cycles did not weaken the material [34].

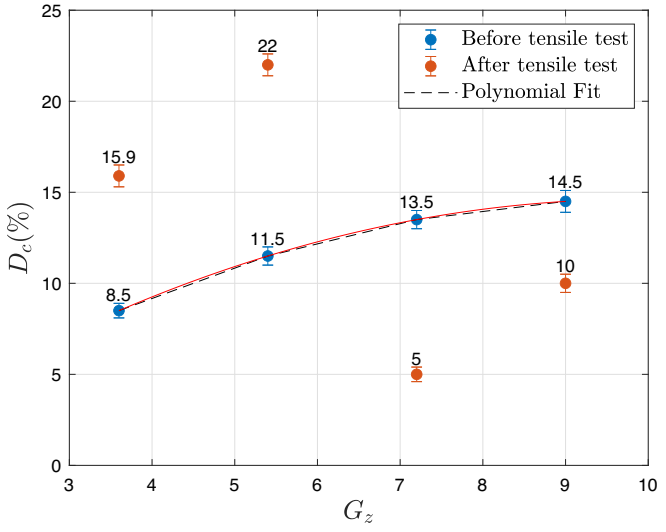

Fig. 4. Relationship between Graetz number (G_z) and degree of crystallinity D_C before (blue dot) and after (orange dot) tensile test. The red line is a polynomial fit that have the scope of guiding the eye.

3.4. Mechanical characterization

Fig. 5a shows three examples of the'P23' type specimen after the printing stage. Fig. 5b captures one specimen after the tensile test. Fig. 5c shows a enlargement of the fracture surface, which allows analysis of the failure characteristics.

The Fig. 7 showcases the temporal power consumption for specimens produced under varying conditions. Notably, the print speed influences the duration of the printing process, with faster speeds leading to shorter print times as evidenced by the blue and purple curves. Moreover, a similar spike pattern in the curves of the samples manufactured $T_p = 40^\circ C$ (yellow and purpule) and $T_p = 80^\circ C$ (Ornge and blue) can be attributed to the binary logic control mechanism of the printer firmware, which does not use a PID to control the plate temperature, but only an on/off logic due to the high thermal inertia of the plate.

The mechanical response of the 3D printed specimens under tensile load is depicted in Fig. 8. Here are presented as example three type of specimens P1, P9, and P17 that are manufactured with the same $T_p = 40^\circ C$ and the same $S_p = 40 mm s^{-1}$, but with different $T_p = 250, 260, 270^\circ C$. The plot displays the variability between three repeated measurements for each set of specimens through a shaded area around the line plot, this shaded region indicates the range of error in the measurements. It is important to note that the elastic modulus, and the maximum stress decrease as the extrusion temperature increases, highlighting the critical role of temperature in the mechanical properties of the recycled PET.

3.5. Multivariate analysis

The Table 5 presents the results of a all the experiments labeled P1 through P24 conducted, to understand the influence of the printing parameters (T_e, T_p, S_p) on energy consumption and mechanical properties (maximum load F_{max}, maximum stress σ_{max}, and maximum longitudinal elastic modulus E_{max}). Multivariate plots were created for energy consumption Fig. 9a, maximum stress Fig. 9b, and Elastic modulus Fig. 9c.

In the Fig. 9a there is a clear increase in energy consumption with higher T_e especially at a, $T_p = 80^\circ C$. This suggests that higher plate temperatures necessitate greater energy expenditure, impacting the cost-effectiveness and sustainability of the printing process. In Fig. 9b a trend of decreasing maximum stress with increasing extrusion temperature is observed, this trend is more pronounced at a $T_p = 80^\circ C$. The same trand is also confirmed by the degree of cristallinity in Fig. 4. In Fig. 9c a descending trand in the elastic modulus with increasing extrusion temperatures, which correlates with the trends observed in the

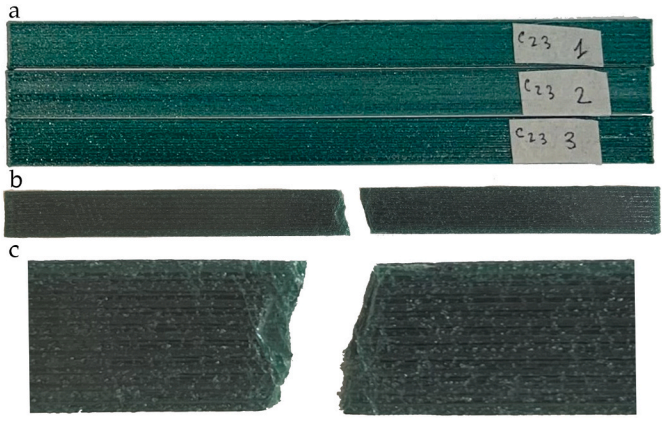

Fig. 5. (a) Shows three 3D-printed tensile test samples labeled P23, (b) displays a specimen post-tensile test with evident separation, and (c) is a close-up of the fracture surface revealing the failure pattern.

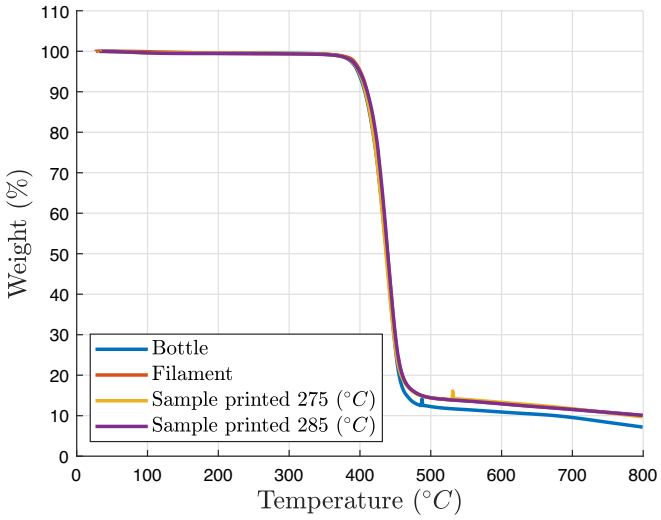

Fig. 6. Thermogravimetric curves of PET in nitrogen, the colors represent the different samples: bottle bottle (red line), filament (grey line), sample printed at $T_p = 275^{\circ}$C (yellow line) and at $T_p = 285^{\circ}$C (yellow line).

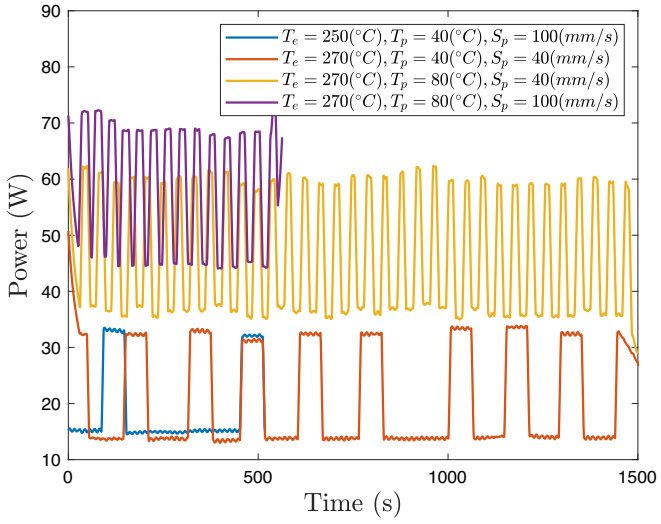

Fig. 7. Power consumption profiles over time for four 3D-printed specimens under different printing parameters.

maximum stress plot. Upon examining Table 5, it is evident that specimens P3, P4, P11, P12, P15, and P16, which were produced at a lower plate temperature of 40 °C with higher print speeds, exhibited higher tensile strengths and energy efficiencies. In contrast, specimens P5, P6, P7, and P8 were printed at a higher plate temperature of 80 °C with slower print speeds. As a result, they exhibited lower mechanical properties and higher energy consumption.

The results explore the effects of these parameters showing variations across different settings, indicating how each parameter influences the final mechanical performance and energy efficiency of the specimens, highlighting the importance of optimizing production parameters to enhance material properties while minimizing energy consumption.

4. Discussion

After characterising the mechanical and energetic consumption of the printed specimens, it is possible to identify a compromise value between the energy and the stain value of the specimens. The accompanying graph in Fig. 10 presents an analysis that identifies the printing

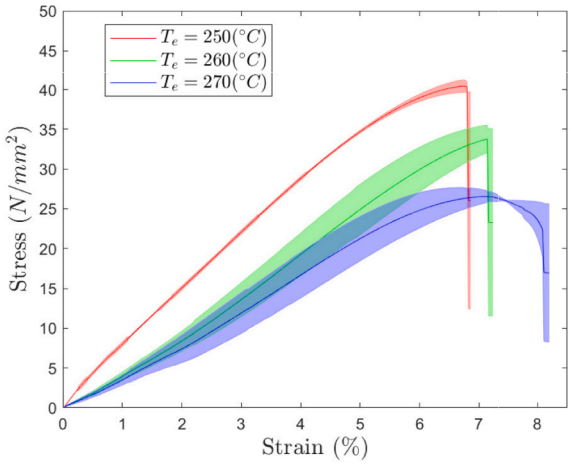

Fig. 8. Stress-strain curves for tensile test specimens P1, P9, P17, manufactured at $T_p = 40^{\circ}$C and $S_p = 40\text{mm}\,\text{s}^{-1}$, with $T_p = 250, 260, 270^{\circ}$C.

parameter combination that achieves an optimal trade-off between mechanical properties and energy consumption.

The graph in Fig. 10 categorizes the performance of the specimens into four distinct regions, based on their energy consumption and mechanical strength. The Best Case region that is the bottom-right quadrant is characterized by a favorable balance where the specimens exhibit 80% of the maximum σ_{max} while maintaining the 20% lowest energy consumption. This is indicative of an optimal parameter combination that yields strong mechanical properties without excessive energy use. The Best Case specimen was manufactured using the following parameters: $T_e = 250^{\circ}\text{C}, T_p = 40^{\circ}\text{C}, S_p = 100(\text{mm}\,\text{s}^{-1})$. In contrast, the Worst Case region that is the top-right quadrant, is marked by specimens that consume a large amount of energy but still display the lowest σ values, representing a low-efficiency outcome. The Worst case specimen was manufactured using the following parameters: $T_e = 270^{\circ}\text{C}, T_p = 80^{\circ}\text{C}$, $S_p = 40\text{mm}\,\text{s}^{-1}$. The bottom-left quadrant represents low energy consumption coupled with low mechanical strength. The graph clearly indicates that specimens processed at an extrusion temperature of 250 °C and a plate temperature of 40 °C fall into the'Best Case' region.

The results are consistent with the analysis of crystallinity discussed in Chapter 3.3. This suggests that S_p directly affects the degree of crystallinity, which in turn impacts the material's strength and thermal stability. Our study highlights a trade-off between crystallinity and energy consumption, underscoring the need for optimized process parameters. Increasing S_p results in higher crystallinity and improved mechanical properties but lower energy consumption. This suggests that these processing conditions are most conducive for achieving an efficient trade-off, optimizing both the energy usage and the mechanical performance of the 3D printed specimens. Recycling PET, especially through AM, offers significant advantages in terms of energy savings, cost reduction, and environmental impact. The energy required to produce secondary plastic from recycled PET is significantly lower than that needed for virgin plastic. Specifically, the energy required for handling and preparing raw materials for primary plastic production is very high, resulting in a 78% difference in energy consumption favoring recycled PET. [24]. The environmental benefits are also substantial. The CO2 emissions associated with producing virgin PET are approximately 2.78 tons of CO2 per ton of plastic, whereas recycled PET emits only 0.91 tons of CO2 per ton of plastic. This difference translates to considerable cost savings, with the cost of CO2 emissions being $66.72 per ton of virgin PET compared to $21.84 per ton of recycled PET. This significant reduction in CO2 emissions and associated costs underscores the environmental and economic benefits of recycling PET. In-house recycling further enhances these benefits by reducing lead times and mitigating

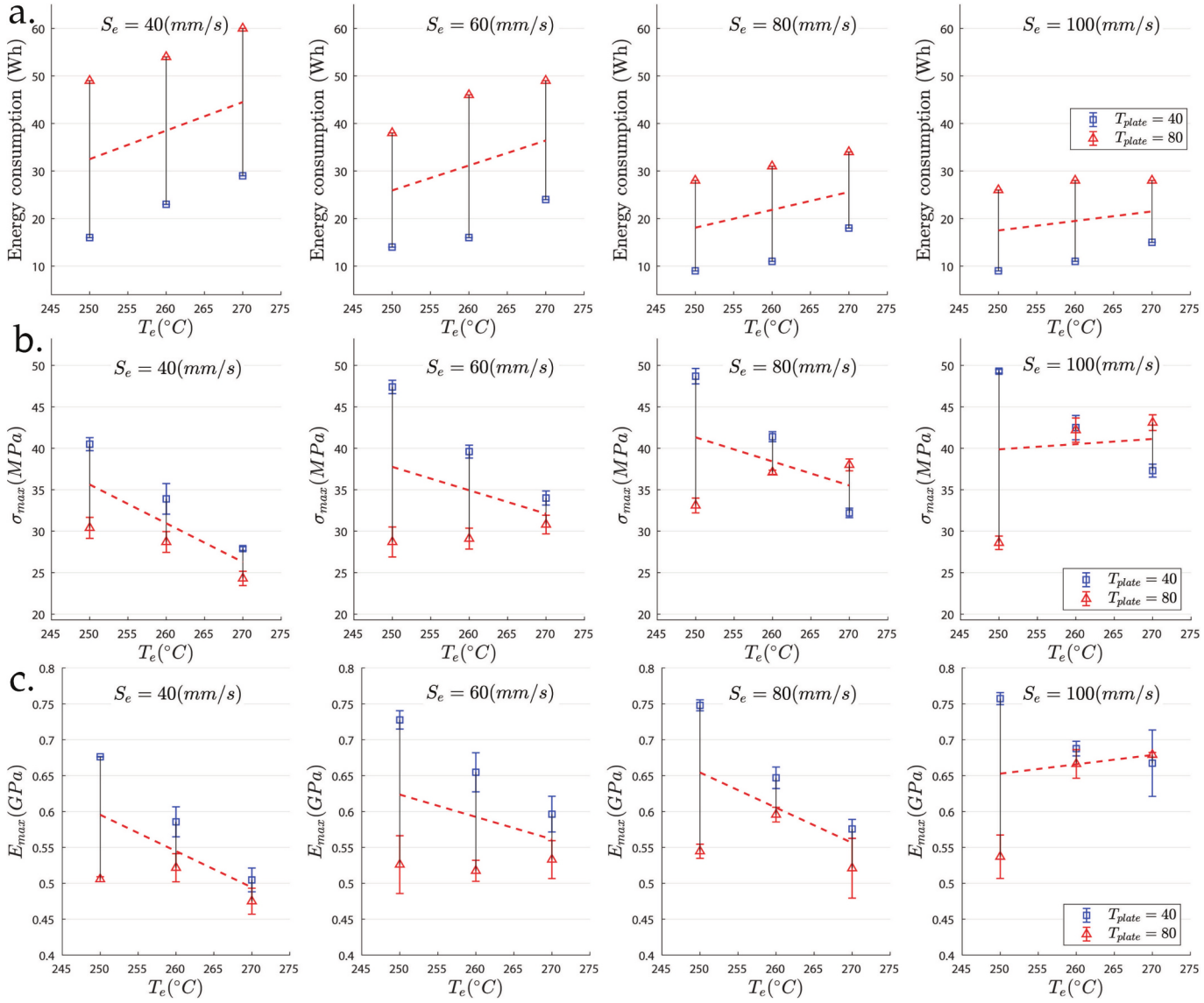

Fig. 9. Multivariate plot of energy consumption (a), tensile modulus (b), elastic modulus (c) for 3D printed specimens demonstrating the effects of (S_e), (T_e), in each plot the red triangles rapresent a $T_p = 80^{\circ}$C, the blue squares a $T_p = 40^{\circ}$C. The error bar is based on the error of three measurements.

supply chain dependencies. By recycling PET on-site, organizations can bypass the complexities and delays associated with external supply chains. This approach not only reduces shipping costs and CO2 emissions but also accelerates production cycles. Moreover, AM itself presents several advantages. It generates minimal waste compared to traditional manufacturing processes and allows for the production of complex geometries that would be difficult or impossible to achieve with conventional methods. These benefits make AM a highly efficient and flexible manufacturing process that complements the sustainability goals of recycling PET. This research also highlights that the optimal process parameters for maximizing the mechanical performance of PET specimens also coincide with the parameters that minimize energy consumption. PET, as a widespread polymer, is notable for its high mechanical properties, ease of printing, and economic viability. These characteristics make it an ideal candidate for recycling and AM, supporting its widespread adoption in various applications. However, it is important to note that the costs associated with in-house recycling, as presented in this study, need to be scaled for industrial activities. While the research demonstrates the feasibility and benefits of on-site recycling in a laboratory setting, translating these findings to an industrial scale will require careful consideration of the economic and logistical challenges involved. Scaling up the process will involve additional investments in equipment, infrastructure, and workforce training, as well as ensuring the consistency and quality of the recycled materials on a larger scale. When comparing the mechanical properties of RPET with those of other recycled polymers studied in the literature, RPET demonstrates superior performance. Vishal M. et al. [35] studied virgin and recycled ABS, reporting maximum strengths at break of 39.19 MPa and 30.7 MPa, respectively, and elastic moduli of 1.36 GPa and 1.12 GPa, respectively. Ana C. Pinho et al. [36] investigated virgin and recycled PLA, finding maximum strengths at break of 20.9 MPa and 39.6 MPa, respectively, and elastic moduli of 12.2 GPa and 15.4 GPa, respectively. Interestingly, the recycling process for crystalline polymers such as PLA can improve the degree of crystallinity, thereby enhancing their mechanical performance. In comparison, the maximum strength and elastic modulus of RPET in this research are 49.3 MPa and 0.76 GPa, respectively. These values indicate that RPET exhibits higher maximum strength than both virgin and recycled ABS and PLA, although its elastic modulus is lower.

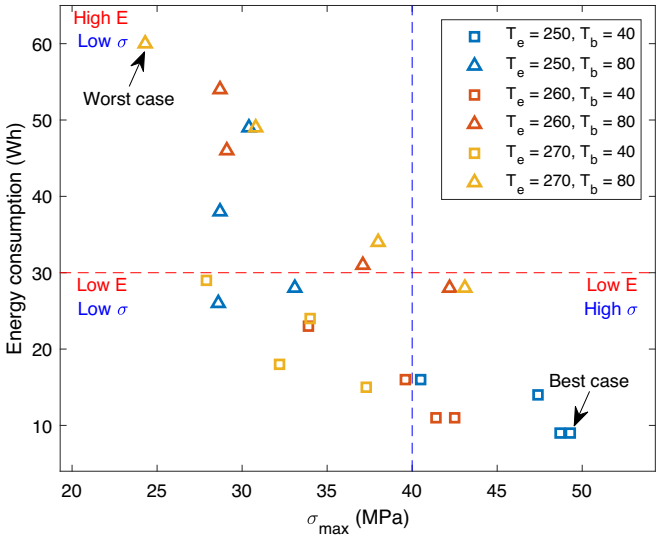

Fig. 10. Energy consumption vs. mechanical strength performance regions for 3D printed specimens.

5. Conclusions

The study explores the optimization of the recycling process for PET using AM, with a focus on energy efficiency and mechanical property enhancement. The results show that the MEX process parameters have a significant impact on the mechanical, thermal properties and energy consumption of the recycling proces of PET in AM. For instance, the use of optimal printing conditions, identified through a DoE, resulted in a significant improvement in mechanical properties confirmed by the literature that report a tensile strength ranging from 40 to 50 MPa [37,38]. In the present study the optimal process parameters were found, specimens manufactured under those conditions showed: 20% increase in tensile strength compared to those produced under less ideal parameters; 30% reduction in the overall energy consumption. The "P4" specimen manufactured with $T_e = 250^{\circ}\mathrm{C}, T_p = 40^{\circ}\mathrm{C}, S_p = 100\mathrm{mm\,s^{-1}}$ report:

$F_{max} = 2237\mathrm{N}$

$\sigma_{max} = 49.3\mathrm{MPa}$

$E_{max} = 0.76\mathrm{GPa}$

Energy = 9Wh

This research highlights the significance of a multi-objective optimization approach in promoting sustainable manufacturing practices. It demonstrates a way to efficiently recycle PET materials and reduce the environmental impact of plastic waste. As highlighted by Pintos et al. [16], R-PET is a promising material for LFAM. Future research could investigate the optimal process parameters that maximize the relationship between consumption and mechanical performance, even when using R-PET with LFAM.

The findings of this study align with those of other studies in the field. For instance, Vidakis et al. [28] explored the energy consumption and mechanical performance in MEX 3D printing of polyamide 6 (PA6) and found that optimizing control settings can significantly impact energy efficiency and mechanical strength. Similarly, another study by Vidakis et al. [39] focused on polylactic acid (PLA) and highlighted the trade-offs between energy consumption and mechanical performance, emphasizing the importance of printing speed and layer thickness as critical factors. Furthermore, Vidakis et al. [40] investigated the mechanical performance over energy expenditure in MEX 3D printing of polycarbonate. Their study demonstrated the significance of optimizing infill density and layer thickness to achieve a balance between energy consumption and mechanical properties. Future research should investigate the influence of additional process parameters, such as bead dimensions (layer height and width), to further optimize mechanical properties and energy efficiency. Conducting a Life Cycle Assessment (LCA) of the process would provide a comprehensive understanding of its environmental impact. Additionally, studying the influence of annealing post-processing on the mechanical properties of recycled PET parts could reveal potential improvements in material performance. Extending the research to include the recycling of HDPE bottle caps and exploring the recycling of mixed PET bottles from different sources would broaden the applicability and impact of these findings [41]. Moreover, exploring the feasibility of recycling the entire bottle by

Table 5
Specimen type, production parameter and results of energy measurement and tensile tests. F_{max} = maximum load, σ_{max} = maximum stress, E_{max} = maximum longitudinal elastic modulus.

Type	T_e (°C)	T_p (°C)	S_p (mm s^{-1})	Energy (Wh)	m_{avg} (g)	F_{max} (N)	σ_{max} (MPa)	E (GPa)
P1	250	40	40	16	9.10 ± 0.49	1786.4 ± 16.35	40.5 ± 1.29	0.68 ± 0.00
P2	250	40	60	14	9.92 ± 0.04	2115.9 ± 122.2	47.4 ± 1.38	0.73 ± 0.02
P3	250	40	80	9	10.30 ± 0.03	2146.9 ± 20.25	48.7 ± 1.57	0.75 ± 0.01
P4	250	40	100	9	10.23 ± 0.03	2237 ± 72.1	49.3 ± 0.37	0.76 ± 0.01
P5	250	80	40	49	7.88 ± 0.05	1402 ± 114.65	30.4 ± 2.19	0.51 ± 0.01
P6	250	80	60	38	8.33 ± 0.05	1343.4 ± 113	28.7 ± 2.71	0.53 ± 0.07
P7	250	80	80	28	8.65 ± 0.04	1483 ± 71.15	33.1 ± 1.43	0.54 ± 0.02
P8	250	80	100	26	8.53 ± 0.03	1391.8 ± 33.1	28.6 ± 1.27	0.54 ± 0.05
P9	260	40	40	23	10.00 ± 0.04	1615.1 ± 112.25	33.9 ± 3.11	0.59 ± 0.03
P10	260	40	60	16	9.41 ± 0.04	1944.9 ± 124.2	39.6 ± 1.20	0.65 ± 0.05
P11	260	40	80	11	8.68 ± 0.03	1944.6 ± 34.4	41.4 ± 1.04	0.65 ± 0.03
P12	260	40	100	11	10.35 ± 0.02	2052.4 ± 54.2	42.5 ± 2.50	0.69 ± 0.02
P13	260	80	40	54	9.78 ± 0.02	1246.1 ± 167.95	28.7 ± 1.97	0.52 ± 0.03
P14	260	80	60	46	8.77 ± 0.02	1439.5 ± 74.05	29.1 ± 2.16	0.52 ± 0.03
P15	260	80	80	31	9.49 ± 0.03	1799.9 ± 28.2	37.1 ± 0.43	0.60 ± 0.02
P16	260	80	100	28	9.62 ± 0.03	1924.8 ± 62.8	42.2 ± 2.41	0.67 ± 0.03
P17	270	40	40	29	9.51 ± 0.02	1296 ± 67.85	27.9 ± 0.40	0.50 ± 0.03
P18	270	40	60	24	10.10 ± 0.02	1544.7 ± 60.15	34 ± 1.33	0.60 ± 0.04
P19	270	40	80	18	10.15 ± 0.01	1513.1 ± 43.55	32.2 ± 0.92	0.58 ± 0.02
P20	270	40	100	15	9.16 ± 0.02	1697.3 ± 83.05	37.3 ± 1.31	0.67 ± 0.08
P21	270	80	40	60	9.99 ± 0.01	1194.4 ± 64.2	24.3 ± 1.45	0.48 ± 0.03
P22	270	80	60	49	9.75 ± 0.02	1523.8 ± 67.5	30.8 ± 1.78	0.53 ± 0.05
P23	270	80	80	34	8.56 ± 0.03	1843.3 ± 20.2	38 ± 1.23	0.52 ± 0.07
P24	270	80	100	28	9.92 ± 0.01	2164.8 ± 105.95	43.1 ± 1.6	0.68 ± 0.01

mixing HDPE from the caps with PET from the bottles could open new avenues for comprehensive recycling strategies. This integrated approach could potentially enhance the versatility and sustainability of recycling practices, making it possible to utilize the full range of materials present in consumer packaging [42]. Future studies could also explore the cyclic recycling of PET, providing guidelines for those intending to reuse the same quantity of material multiple times, thereby extending its life cycle and maximizing its utility. By addressing these areas, future studies can enhance the sustainability and efficiency of recycling processes, contributing to a more robust and comprehensive approach to AM with recycled materials. This research stands out by offering a comprehensive, multi-objective approach that addresses energy consumption, recycling efficiency, and the mechanical and thermal properties of recycled materials in AM. By simultaneously considering these factors, the study bridges a critical gap in the literature, providing a holistic view that enhances the sustainability and efficiency of recycling and manufacturing processes. The approach emphasizes the benefits of on-site recycling, aiming to reduce the environmental footprint by transforming plastic waste into valuable products directly at the point of origin. This scalable and eco-friendly methodology leverages the abundant availability of discarded plastics, contributing to a more sustainable and circular economy.

CRediT authorship contribution statement

Luca Landolfi: Writing – review & editing, Writing – original draft, Visualization, Validation, Resources, Methodology, Investigation, Formal analysis, Data curation, Conceptualization. **Andrea Lorenzo Henri Sergio Detry:** Writing – review & editing, Writing – original draft, Visualization, Validation, Resources, Methodology, Investigation, Formal analysis, Data curation, Conceptualization. **Ersilia Cozzolino:** Writing – review & editing, Writing – original draft, Visualization, Formal analysis, Data curation. **Daniele Tammaro:** Writing – review & editing, Validation, Supervision, Formal analysis, Data curation, Conceptualization. **Antonino Squillace:** Writing – review & editing, Supervision, Project administration, Conceptualization.

Declaration of competing interest

The authors declare that they have no known competing financial interests or personal relationships that could have appeared to influence the work reported in this paper.

Data availability

Data will be made available on request.

Acknowledgements

The authors would like to thank Antonio Gallo, for his support in experimental activities, Giovanna Giuliana Buonocore of the Institute of Polymers, Composites and Biomaterials of the Italian National Research Council for their support and resources in carrying out some tests, and Antonello Astartita, for insightful discussions on the data collected and the conceptualization. This work was supported by the Italian Ministry of Research financing the Fit for Medical Robotics (Fit4MedRob), Grant PNRR PNCO000007, and 3D-Printed Nanocomposite Metamaterials by Foaming and Additive Manufacturing In-Line (3D FAMIL), Grant PRIN2022 2022FMKAAM.

References

[1] T.O. Wiedmann, H. Schandl, M. Lenzen, D. Moran, S. Suh, J. West, K. Kanemoto, The material footprint of nations, Proc. Natl. Acad. Sci. 112 (20) (2015) 6271–6276.
[2] European Commission, Roadmap to a resource efficient europe. com (2011) 571 final, 2011.
[3] S. Bringezu, R. Bleischwitz, Sustainable Resource Management: Global Trends, Visions and Policies, Routledge, 2017.
[4] H. Wu, H. Mehrabi, P. Karagiannidis, N. Naveed, Additive manufacturing of recycled plastics: strategies towards a more sustainable future, J. Clean. Prod. 335 (2022) 130236.
[5] A. Vozniak, R. Hosseinnezhad, I. Vozniak, A. Galeski, Pet mechanical recycling. A new principle for chain extender introduction, Sustain. Mater. Technol. 40 (2024) e00886.
[6] M.Y. Khalid, Z.U. Arif, W. Ahmed, H. Arshad, Recent trends in recycling and reusing techniques of different plastic polymers and their composite materials, Sustain. Mater. Technol. 31 (2022) e00382.
[7] F.A.C. Sanchez, H. Boudaoud, M. Camargo, J.M. Pearce, Plastic recycling in additive manufacturing: a systematic literature review and opportunities for the circular economy, J. Clean. Prod. 264 (2020) 121602.
[8] C. Baechler, M. DeVuono, J.M. Pearce, Distributed recycling of waste polymer into reprap feedstock, Rapid Prototyp. J. 19 (2) (2013) 118–125.
[9] S.C. Dertinger, N. Gallup, N.G. Tanikella, M. Grasso, S. Vahid, P.J. Foot, J. M. Pearce, Technical pathways for distributed recycling of polymer composites for distributed manufacturing: windshield wiper blades, Resour. Conserv. Recycl. 157 (2020) 104810.
[10] B. Peeters, N. Kiratli, J. Semeijn, A barrier analysis for distributed recycling of 3d printing waste: taking the maker movement perspective, J. Clean. Prod. 241 (2019) 118313.
[11] S. Halassi, J. Semeijn, N. Kiratli, From consumer to prosumer: a supply chain revolution in 3d printing, Int. J. Phys. Distrib. Logist. Manag. 49 (2) (2019) 200–216.
[12] H.A. Colorado, E.I.G. Velásquez, S.N. Monteiro, Sustainability of additive manufacturing: the circular economy of materials and environmental perspectives, J. Mater. Res. Technol. 9 (4) (2020) 8221–8234.
[13] T. Peng, K. Kellens, R. Tang, C. Chen, G. Chen, Sustainability of additive manufacturing: an overview on its energy demand and environmental impact, Addit. Manuf. 21 (2018) 694–704.
[14] Y. Wang, T. Peng, Y. Xiong, S. Kim, Y. Zhu, R. Tang, An ontology of eco-design for additive manufacturing with informative sustainability analysis, Adv. Eng. Inform. 60 (2024) 102430.
[15] A. Schwarz, T. Ligthart, D. Godoi Bizarro, P. De Wild, B. Vreugdenhil, T. van Harmelen, Plastic recycling in a circular economy; determining environmental performance through an lca matrix model approach, Waste Manag. 121 (2021) 331–342.
[16] P. Burgos Pintos, A. Sanz de León, S.I. Molina, Large format additive manufacturing of polyethylene terephthalate (pet) by material extrusion, Addit. Manuf. 79 (2024) 103908.
[17] N. Vidakis, M. Petousis, L. Tzounis, S. Grammatikos, E. Porfyrakis, A. Maniadi, N. Mountakis, Sustainable additive manufacturing: mechanical response of polyethylene terephthalate glycol over multiple recycling processes, Materials 14 (2021) 03.
[18] N. Vidakis, M. Petousis, L. Tzounis, A. Maniadi, E. Velidakis, N. Mountakis, J. Kechagias, Sustainable additive manufacturing: Mechanical response of polyamide 12 over multiple recycling processes, Materials 14 (2021) 466.
[19] J. Kechagias, S. Zaoutsos, Effects of 3d-printing processing parameters on fff parts' porosity: outlook and trends, Mater. Manuf. Process. 39 (2024) 01.
[20] J. Kechagias and S. Zaoutsos, "An investigation of the effects of ironing parameters on the surface and compression properties of material extrusion components utilizing a hybrid-modeling experimental approach," Progress in Additive Manufacturing, 11 2023.
[21] J. Kechagias, D. Chaidas, Fused filament fabrication parameter adjustments for sustainable 3d printing, Mater. Manuf. Process. 02 (2023).
[22] N. Fountas, S. Zaoutsos, D. Chaidas, J. Kechagias, N. Vaxevanidis, Statistical modelling and optimization of mechanical properties for pla and pla/wood fdm materials, Mater. Today Proc. 93 (2023) 08.
[23] N. Vidakis, J. Kechagias, M. Petousis, F. Vakouftsi, N. Mountakis, The effects of fff 3d printing parameters on energy consumption, Mater. Manuf. Process. 38 (2022) 07.
[24] H. Liu, K. Gong, A. Portela, V. Chyzna, G. Yan, Z. Cao, R. Dunbar, Y. Chen, Investigation of distributed recycling of polylactic acid over multiple generations via the granule-based material extrusion process, J. Clean. Prod. 436 (2024) 140609.
[25] H. Schneevogt, K. Stelzner, B. Yilmaz, B.E. Abali, A. Klunker, C. Völlmecke, Sustainability in additive manufacturing: exploring the mechanical potential of recycled pet filaments, Composites Adv. Mater. 30 (2021), 26349833211000063.
[26] D. Vaes, P. Van Puyvelde, Semi-crystalline feedstock for filament-based 3d printing of polymers, Prog. Polym. Sci. 118 (2021) 101411.
[27] E. Gothár, H. Schanz, Bringing a governance perspective to plastic litter: a structural analysis of the german pet industry, Sustainable Production and Consumption 31 (2022) 630–641.
[28] C. David, D. Sagris, M. Petousis, N.K. Nasikas, A. Moutsopoulou, E. Sfakiotakis, N. Mountakis, C. Charou, N. Vidakis, Operational performance and energy efficiency of mex 3d printing with polyamide 6 (pa6): multi-objective optimization of seven control settings supported by l27 robust design, Appl. Sci. 13 (15) (2023).
[29] M. Alzahrani, H. Alhumade, L. Simon, C. Madhuranthakam, A. Elkamel, Additive manufacture of recycled poly(ethylene terephthalate) using pyromellitic dianhydride targeted for fdm 3d-printing applications, Sustainability 15 (2023) 5004.
[30] J. Butt, R. Bhaskar, V. Mohaghegh, Analysing the effects of layer heights and line widths on fff-printed thermoplastics, Int. J. Adv. Manuf. Technol. 121 (11–12) (2022) 7383–7411.

[31] D. Tammaro, R. Della Gatta, M.M. Villone, P.L. Maffettone, Continuous 3d printing of hierarchically structured microfoamed objects, Adv. Eng. Mater. 24 (5) (2022) 2101226.
[32] B. Van de Voorde, A. Katalagarianakis, S. Huysman, A. Toncheva, J.-M. Raquez, I. Duretek, C. Holzer, L. Cardon, K.V. Bernaerts, D. Van Hemelrijck, L. Pyl, S. Van Vlierberghe, Effect of extrusion and fused filament fabrication processing parameters of recycled poly(ethylene terephthalate) on the crystallinity and mechanical properties, Addit. Manuf. 50 (2022) 102518.
[33] D. Kawakami, B.S. Hsiao, C. Burger, S. Ran, C. Avila-Orta, I. Sics, T. Kikutani, K. I. Jacob, B. Chu, Deformation-induced phase transition and superstructure formation in poly(ethylene terephthalate), Macromolecules 38 (1) (2005) 91–103.
[34] J. Badia, A. Martinez-Felipe, L. Santonja-Blasco, A. Ribes-Greus, Thermal and thermo-oxidative stability of reprocessed poly(ethylene terephthalate), J. Anal. Appl. Pyrolysis 99 (2013) 191–202.
[35] V. Mishra, C.K. Ror, S. Negi, S. Kar, L.N. Borah, 3d printing with recycled abs resin: effect of blending and printing temperature, Mater. Chem. Phys. 309 (2023) 128317.
[36] A.C. Pinho, A.M. Amaro, A.P. Piedade, 3d printing goes greener: study of the properties of post-consumer recycled polymers for the manufacturing of engineering components, Waste Manag. 118 (2020) 426–434.
[37] M. Bustos Seibert, G.A. Mazzei Capote, M. Gruber, W. Volk, T.A. Osswald, Manufacturing of a pet filament from recycled material for material extrusion (mex), Recycling 7 (5) (2022).
[38] N.E. Zander, M. Gillan, R.H. Lambeth, Recycled polyethylene terephthalate as a new fff feedstock material, Addit. Manuf. 21 (2018) 174–182.
[39] N. Vidakis, M. Petousis, E. Karapidakis, N. Mountakis, C. David, D. Sagris, Energy consumption versus strength in mex 3d printing of polylactic acid, Adv. Ind. Manufacturing Eng. 6 (2023) 100119.
[40] N. Vidakis, M. Petousis, C.N. David, D. Sagris, N. Mountakis, E. Karapidakis, Mechanical performance over energy expenditure in mex 3d printing of polycarbonate: a multiparametric optimization with the aid of robust experimental design, J. Manufact. Mater. Processing 7 (1) (2023).
[41] E.B. Mejia, S. Al-Maqdi, M. Alkaabi, A. Alhammadi, M. Alkaabi, N. Cherupurakal, A.-H.I. Mourad, Upcycling of hdpe waste using additive manufacturing: Feasibility and challenges, 2020 Adv Sci. Eng. Technol. International Conf. (ASET) (2020) 1–6.
[42] T.T.G. Rashwan Ola, Koroneos Zachary, Extrusion and characterization of recycled polyethylene terephthalate (rpet) filaments compounded with chain extender and impact modifiers for material-extrusion additive manufacturing. 2020 Advances in Science and Engineering Technology International Conferences (ASET), 2023.